Identification of in vivo phosphorylation sites of lens proteins from porcine eye lenses by a gel-free phosphoproteomics approach

Shyh-Horng Chiou,[1,2] Chun-Hao Huang,[1,2] I-Liang Lee,[1,2] Yi-Ting Wang,[3] Nai-Yu Liu,[4] Yeou-Guang Tsay,[4] Yu-Ju Chen[3]

(Chun-Hao Huang, I-Liang Lee, and Yi-Ting Wang contributed equally to this paper)

[1]*Graduate Institute of Medicine and Center for Research Resources and Development, Kaohsiung Medical University, Kaohsiung, Taiwan;* [2]*Institute of Biological Chemistry, Academia Sinica, Taipei, Taiwan;* [3]*Institute of Biochemical Sciences, National Taiwan University, Taipei; Chemical Biology and Molecular Biophysics Program, Taiwan International Graduate Program, Institute of Chemistry, Academia Sinica, Taipei, Taiwan;* [4]*Institute of Biochemistry and Molecular Biology, National Yang-Ming University, Taipei, Taiwan*

Purpose: Phosphorylation is an important post-translational modification for the cellular regulation of various biosignaling pathways. We have identified in vivo phosphorylation sites of various lens proteins including especially the major structural proteins of the crystallin family from porcine eye lenses by means of two-dimensional gel electrophoresis (2-DE) or immobilized metal affinity chromatography (IMAC) followed by liquid chromatography coupled with tandem mass spectrometry (LC-MS/MS).

Methods: For the identification of phosphorylated residues in various lens proteins of porcine lens extracts, we have adapted two complementary proteomic approaches, i.e., pre-fractionation of protein samples with 2-DE or enrichment of phosphopeptides with IMAC followed by LC-MS/MS analysis and database search. The results were compared and validated with those in phosphoproteomics databases.

Results: Two subunits of α-crystallin, αA-crystallin and αB-crystallin, as well as other lens crystallins and non-crystallin cellular proteins, such as β-enolase, heat shock protein β-1 (HSP27), and glucose-6-phosphate isomerase (GPI) were found to be phosphorylated in vivo at specific sites. Moreover, αA- and αB-crystallins were found to be the most abundantly phosphorylated proteins in porcine lenses, being extensively phosphorylated on serine or threonine, but not on tyrosine residues.

Conclusions: The complementary gel-based and gel-free proteomic strategies have been compared and evaluated for the study of crystallin phosphorylation from whole tissue extracts of porcine eye lenses. Technically, the IMAC method facilitates direct site-specific identification of phosphorylation residues in lens proteins, which does not necessitate the pre-MS/MS 2-DE separation of protein samples. Moreover, the improved strategy using gel-free phosphoproteomics analysis affords a more effective and simplistic method for the determination of in vivo phosphorylation sites than the conventional 2-DE pre-separation of protein mixture. This study should form a firm basis for the comprehensive analysis of post-translational modification of lens proteins in terms of aging or various diseased states.

Mammalian eye lenses are composed of elongated fiber cells, of which approximately 90% of the total soluble proteins belong to three major classes of proteins, i.e., α−, β−, and γ −crystallins [1,2]. Essentially, these crystallins can exist in the eye lens with little turnover throughout the entire lifespan, albeit with various degrees of post-translational modifications such as deamidation, phosphorylation, and proteolytic truncation [3-5]. Among these, phosphorylation is most noteworthy for playing a major role in the regulation of various biosignaling pathways [6] which may include cancer development, aging, and cataract formation. Therefore

identification of protein phosphorylation and its exact locations in proteins or enzymes of interest are always considered as a preeminent and nontrivial task in the conventional mechanistic and functional study of various cellular proteins. Mainly attributable to the advent of emerging proteomics, the investigation of protein phosphorylation has recently become less tedious and more amendable to routine analysis [7].

The common strategy of most conventional proteomic approaches to the identification of proteins rests in the peptide mass fingerprints of proteins under study, which can be used as an identification tag to search the corresponding identical or highly homologous sequence fragment patterns in protein sequence databank. Such fingerprints usually come from the tandem mass spectra of peptides generated from proteolytic digestion of proteins of interest. However before obtaining the

Correspondence to: Shyh-Horng Chiou, Center for Research Resources and Development, Kaohsiung Medical University, Kaohsiung 807 or Institute of Biological Chemistry, Academia Sinica, Taipei 115, Taiwan; Phone: (886)-7-3133874; FAX: (886)-7-3133434; email: shchiou@kmu.edu.tw

digested protein fragments, the global or comprehensive separation of a given protein mixture is generally required. 2-DE gel electrophoresis was previously considered as the method of choice, as it could afford a high throughput and relatively high-resolution analytical tool to resolve and separate a mixture of thousands of protein species with different charge and size properties [8]. However, the serious drawback of low sensitivity and under-representation for some special classes of proteins such as the extremely basic or acidic groups of proteins and membrane proteins [8,9] necessitated the development of more sensitive labeling methods such as stable isotopic labeling [10] in conjunction with multidimensional LC-MS/MS analysis. Thus, direct digestion of total cellular protein extracts followed by high-resolution LC-MS/MS, the so-called shotgun strategy, has been shown to facilitate the highly sensitive identification of protein mixtures without prior protein separation on 2-DE gels [7,11,12].

In spite of the rapid improvement of various types of mass spectrometry designed to study post-translational modifications of cellular proteins, especially concerning protein phosphorylation, there still exist some discrepancies or ambiguities between results obtained from previous investigations of different laboratories. The major emphasis of recent proteomic studies is being directed toward a more facile and global analysis of cellular systems, however methodologies to date still do not exist for conducting a routine and reliable high-throughput analysis of proteome-wide changes in the phosphorylation of proteins. In this study, phosphorylated and nonphosphorylated lens proteins from porcine eye lenses were identified by gel-based 2-DE protein fractionation and gel-free enrichment of phosphopeptides from trypsin-digested protein mixture on immobilized metal affinity chromatography (IMAC), followed by LC-MS/MS. Based on our results of the comparison and evaluation of two different protocols of proteomic approaches, we conclude that gel-free IMAC phosphopeptide enrichment, coupled with LC-MS/MS analysis, is now capable of identification of phosphorylated sites from the whole lens extract, effectively circumventing the need for prior protein separation by two-dimensional gel electrophoresis.

METHODS

Chemicals: Triethylammonium bicarbonate (TEABC) and iron chloride (FeCl₃) were purchased from Sigma Aldrich (St. Louis, MO). The BCA™ protein assay reagent kit was obtained from Pierce (Rockford, IL). Ammonium persulfate and N, N, N', N'-tetramethylenediamine were purchased from Amersham Pharmacia (Piscataway, NJ). Acetic acid (AA) was purchased from J. T. Baker (Phillipsburg, NJ). Trifluoroacetic acid (TFA), formic acid (FA), and HPLC-grade acetonitrile were purchased from Sigma Aldrich (St. Louis, MO). Modified, sequencing-grade trypsin was purchased from Promega (Madison, WI).

Preparation of porcine lens extract: Young porcine eyeballs were obtained from a local slaughterhouse. Eyeballs were kept and stored at −80 °C in a freezer before dissection. Porcine lenses were removed from the eyeballs, homogenized, and suspended in the buffer of 20 mM Tris-HCl, pH 6.8 for the extraction of total lens crystallins as described previously [13-17].

Two-dimensional gel electrophoresis: Porcine lens extract was solubilized in lysis buffer containing 8 M urea, 0.5% CHAPS or Triton X-100. After the estimation of protein content using a 2-D Quant Kit (Amersham Biosciences, Uppsala, Sweden), about 100 μg total protein was loaded onto IPG gel strips (pH 3–10 Nonlinear, 24 cm, Amersham Biosciences, Uppsala, Sweden). The IPG strips were rehydrated overnight according to the operational guideline of the manufacturer (Amersham Biosciences, Uppsala, Sweden). For the first-dimensional separation, isoelectric focusing (IEF) was performed using Ettan IPGphor II (Amersham Biosciences, Uppsala, Sweden) at 20 °C with 300–8,000 V for 16 h. After IEF, the IPG strips were equilibrated for 10 min each in two equilibration solutions (50 mM Tris-HCl, pH 8.8, 6 M urea, 2% SDS, 30% glycerol containing 100 mg dithiothreitol [DTT] or 250 mg iodoacetic acid [IAA], respectively), and then attached to a 12.5% SDS-polyacrylamide gel of Laemmli's buffer system, then covered by 0.5% agarose gel. 2-DE was conducted at 130–250 V for 5–6 h until the bromophenol blue reached the bottom of the gel. The gels were stained by Sypro-Ruby overnight. The protein profiles of the gels were scanned using a Typhoon 9400 scanner (Amersham Biosciences, Uppsala, Sweden). Gel image matching was done using ImageMaster™ 2D Platinum Software Version 5.0 (Amersham Biosciences, Uppsala, Sweden). Intensity levels were normalized between gels as a proportion of the total protein intensity detected for the entire gel.

In-gel digestion: Based on the 2D gel analysis of samples, differentially expressed proteins were selected for further identification by LC-MS/MS. The protein spots were cut from 2D gels, and then destained three times with 25 mM of ammonium bicarbonate buffer (pH 8.0) in 50% acetonitrile (ACN) for 1 h. The gel pieces were dehydrated in 100% ACN for 5 min and then dried for 30 min in a vacuum centrifuge. Enzyme digestion was performed by adding 0.5 μg trypsin in 25 mM of ammonium bicarbonate per sample at 37 °C for 16 h. The peptide fragments were extracted twice with 50 μl 50% ACN/ 0.1% TFA. After removal of ACN and TFA by centrifugation in a vacuum centrifuge, samples were dissolved in 0.1% formic acid as well as 50% ACN.

LC-MS/MS analysis from 2-DE: Electrospray mass spectrometry was performed using a Finnigan LTQ Orbitrap hybrid mass spectrometer interfaced with Agilent 1200 capillary high-performance liquid chromatography (HPLC) system. A 100×0.075 mm Agilent C18 column (3.5 μm

particle diameter) with mobile phases of A (0.1% formic acid in water) and B (0.1% formic acid in acetonitrile) were used. The peptides were eluted at a flow rate of 0.4 μl/min with an acetonitrile gradient, which consisted of 5%–10% B in 5 min, 10%–50% B in 25 min, and 50%–95% B in 4 min. The spectra for the eluting fractions were acquired as successive sets of scan modes. The MS scan determines the intensity of the ions in the m/z range of 200 to 2,000, and a specific ion was selected for a tandem MS/MS scan. The former examined the charge number of the selected ion and the latter acquired the spectrum (CID spectrum or MS/MS spectrum) for the fragment ions derived by collision-induced dissociation. Proteins were identified in NCBI databases by use of MS/MS ion search with the search program Mascot.

Comprehensive PTM mapping analysis: The data interpretation steps were facilitated by Xcalibur and TurboSequest softwares (Thermo electron, san Jose, CA) as well as in-house proprietary programs. Our Excel macro Output Plus can extract MS and MS/MS data and store them as text files. SegMS macro can generate segmental average MS scans using the above MS data. The macro PTMFinder can use the segmental average MS scan and TurboSequest results to screen the likely modification-containing peptides. For modified candidate peptides with acquired MS/MS spectra, we use another macro MS2Graph to verify their identities along with identification of their modified residues within the peptides for further validation.

Gel-assisted digestion: The protein samples from the lens were subjected to gel-assisted digestion. The sample was incorporated into a gel directly in the Eppendorf vial with acrylamide/ bisacrylamide solution (40%, v/v, 29:1), 10% (w/v) APS, 100% TEMED as a proportion (14:5:0.7:0.3) [9,18]. The gel was cut into small pieces and washed several times with 25 mM TEABC containing 50% (v/v) ACN. The gel samples were further dehydrated with 100% ACN and completely dried using SpeedVac. Proteolytic digestion was then performed with trypsin (protein:trypsin=50:1, g/g) in 25 mM TEABC with incubation overnight at 37 °C. The tryptic peptides were dried completely under vacuum and stored at −30 °C.

IMAC Procedure: The IMAC column was first capped at one end with a 0.5 μm frit disk enclosed in a stainless steel column-end fitting. The Ni-NTA resin was extracted from spin column (Qiagen, Hilden, Germany) and packed into a 10 cm microcolumn (500 μm i.d. PEEK column; Upchurch Scientific/ Rheodyne, Oak Harbor, WA) as described previously [19]. Automatic purification of phosphopeptides was performed by connecting to an autosampler and an HP1100 solvent delivery system (Hewlett-Packard, Palo Alto, CA) with a flow rate 13 μl/min. First, the Ni^{2+} ions were removed with 100 μl 50 mM EDTA in 1 M NaCl. Then the IMAC column was activated with 100 μl 0.2 M $FeCl_3$ and equilibrated with loading buffer for 30 min before sample

loading. The loading buffer/ acetic acid was 6% (v/v) and the pH was adjusted to 3.0 with 0.1 M NaOH (pH=12.8). The peptide samples from trypsin digestion were reconstituted in the loading buffer and loaded into the IMAC column that had been equilibrated with the same loading buffer for 20 min. The unbound peptides were then removed with 100 μl of washing solution, consisting of 75% (v/v) loading buffer and 25% (v/v) ACN, followed by equilibration with loading buffer for 15 min. Finally, the bound peptides were eluted with 100 μl 200 mM $NH_4H_2PO_4$ (pH 4.4). Eluted peptide samples were dried under vacuum and then reconstituted in 0.1% (v/v) TFA (40 μl) for further desalting and concentration using ZipTips™ (Millipore, Bedford, CA).

LC-MS/MS analysis from gel-assisted digestion and IMAC: Purified phosphopeptide samples were reconstituted in 4 μl buffer A (0.1% formic acid (FA) in H_2O) and analyzed by LC-Q-TOF MS (Waters Q-TOF™ Premier; Waters Corp, Milford, MA). For LC-MS/MS analysis by Waters Q-TOF™ Premier, samples were injected into a 2 cm×180 μm capillary trap column and separated by 20 cm×75 μm Waters1 ACQUITYTM 1.7 mm BEH C18 column using a nanoACQUITY Ultra Performance LC™ system (Waters Corp.). The column was maintained at 35 °C and bound peptides were eluted with a linear gradient of 0%–80% buffer B (buffer A, 0.1% FA in H_2O; buffer B, 0.1% FA in ACN) for 120 min. MS was operated in ESI positive V mode with a resolving power of 10,000. NanoLockSpray source was used for accurate mass measurement and the lock mass channel was sampled every 30 s. The mass spectrometer was calibrated with a synthetic human [Glu[1]]-Fibrinopeptide B solution (1 pmol/μl, from Sigma Aldrich) delivered through the NanoLockSpray source. Data acquisition was operated in the data directed analysis (DDA). The method included a full MS scan (m/z 400–1,600, 0.6 s) and three MS/MS (m/z 100–1,990, 1.2 s each scan) sequentially on the three most intense ions present in the full scan mass spectrum.

Database search and data-filtering: Raw MS/MS data were converted into peak lists using Distiller (version 2.0; Matrix Science, London, UK) with default parameters. All MS/MS samples were analyzed using Mascot (version 2.2.1; Matrix Science, London, UK). Mascot was set up to search the Swissprot_Mammalia (version 54.2, 55,307 entries) assuming trypsin as the digestion enzyme. Mascot was searched with a fragment ion mass tolerance of 0.1 Da and a parent ion tolerance of 0.1 Da. Two missed cleavages were allowed for trypsin digestion. Phosphorylation (Ser/Thr/Tyr) and oxidation (Met) were selected as variable modifications. To evaluate the false discovery rate of protein identification, we repeated the search using identical search parameters and validation criteria against a randomized decoy database created by Mascot. The false discovery rates with Mascot score >36 (p<0.05) was 0.73% in this study.

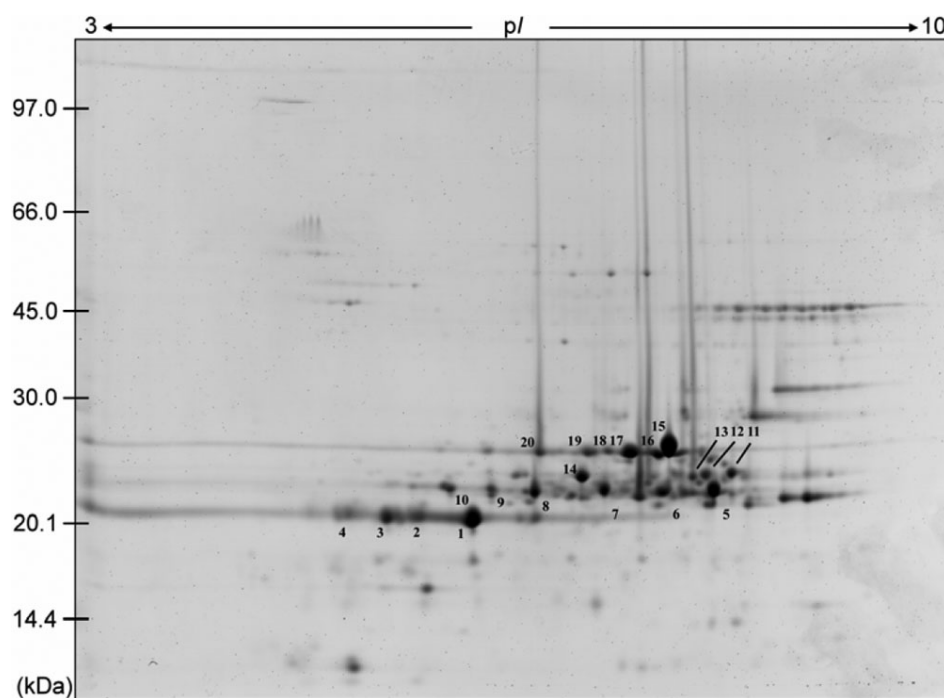Figure 1. 2-DE gel patterns of porcine lens proteins. Total protein (100 μg) in each sample was loaded onto immobilized pH gradient (IPG) gel strips (pH 3–10 Nonlinear, 13 cm). For the first-dimensional separation, IEF was performed using Ettan IPGphor II (Amersham Biosciences) at 300–8,000 V for 16 h. After IEF, the IPG strips were equilibrated in SDS-urea buffer and placed onto the second-dimensional SDS–PAGE. After electrophoresis, the gels were fixed in 10% methanol and 7% acetic acid and stained by Sypro-Ruby. The IPG strips were rehydrated, and after IEF, subjected to 2-DE. Protein spots marked by No. 1–20 on the map were further identified by nano LC-MS/MS and listed in Table 1. It is noteworthy that porcine lenses contain many protein isoforms which present themselves as a series of parallel spots with similar molecular masses in 2-DE profiles. The result is representative of three independent experiments.

RESULTS AND DISCUSSION

The availability of complete genome sequences is moving biologic research to an era where cellular systems are analyzed as a whole rather than as individual components. While global gene expression measurements at the mRNA level opens the door to important biologic advances, much of the understanding of cellular systems and the roles of various cellular constituents still depends on proteomics. The study of proteins at the level of the cellular systems using the current proteomics methodology will provide a firm basis for understanding the complex biosignaling pathways of the whole organism within the interdisciplinary realm of systems biology [20]. Therefore, the global understanding of cellular systems revealed by proteomic investigations will create new avenues of research unlikely to arise from the past paradigm of "single" protein characterization methodologies.

Studies estimate that as many as one-third of all cellular proteins derived from mammalian cells are phosphorylated [6]. Although greater emphasis is being directed toward a comprehensive global analysis of cellular systems, methodologies still do not exist for reliable, high-throughput analysis of proteome-wide changes in the phosphorylation of proteins. Direct determination of individual phosphorylation sites occurring on phosphoproteins in vivo has been difficult to date, typically requiring the purification to homogeneity of the phosphoprotein of interest before analysis. There has been a need for a more rapid and general method for the analysis of protein phosphorylation in complex protein mixtures [21]. In this study, phosphorylated and nonphosphorylated lens proteins from porcine eye lenses were identified and compared by two complementary proteomic protocols, i.e., (1) gel-based 2-DE protein fractionation and (2) gel-free enrichment of phosphopeptides from trypsin-digested protein mixture on immobilized metal affinity chromatography (IMAC) followed by LC-MS/MS. We attempt to evaluate and establish a simplistic protocol to study the post-translational modifications, especially phosphorylation, on the whole lens extract.

Previous reports regarding the investigation of phosphorylation sites of lens crystallins started from the observation that radiolabeled inorganic phosphate (^{32}Pi) could be incorporated into both αA- and αB-crystallins with some evidence that serine was the only phosphorylated residue [22]. In vitro phosphorylation of αB-crystallin was later found to be located principally at Ser-45 and Ser-59 [23], in contrast to the in vivo phosphorylated sites at Ser-19 and Ser-45 [24]. For αB-crystallin in the lens, the major phosphorylation sites have been confirmed to be at serine residues 19, 45, and 59 and the phosphorylation at Ser-45 results in uncontrolled aggregation [4,25]. The phosphorylation of αA-crystallins was also identified by mass spectrometry [26]. Thus, there appeared to be some discrepancies or ambiguities, especially concerning different phosphorylated sites of crystallins under in vivo and in vitro conditions between previous investigations in the literature.

Gel-based proteomic analysis of porcine lens extract: The global protein-expression profile of porcine lens was analyzed using high-resolution 2-DE. The p*I* range for the

TABLE 1. PROTEINS OF PORCINE EYE LENS IDENTIFIED BY 2-DE AND LC-MS/MS ANALYSIS.

Spot	Protein name	Accession number	Mascot Score	pI/mass, kDa	Normalized spot intensity, %	Phosphopeptides
1	αA-crystallin	P02475	536	5.78/19.7	8.9	
2	αA-crystallin	P02475	428	5.78/19.7	3.0	
3	αA-crystallin	P02475	442	5.78/19.7	3.4	
4	αA-crystallin	P02475	272	5.78/19.7	1.8	
5	αB-crystallin	Q7M2W6	438	6.76/20.1	5.4	RPFFPFHSPSR
6	αB-crystallin	Q7M2W6	465	6.76/20.1	2.8	RPFFPFHSPSR
7	αB-crystallin	Q7M2W6	358	6.76/20.1	2.9	
8	βA4-crystallin	XP_001927427	335	5.91/22.4	2.8	
9	βA4-crystallin	XP_001927427	437	5.91/22.4	1.0	
10	βA4-crystallin	XP_001927427	351	5.91/22.4	0.9	
11	βB3-crystallin	XP_001929508	390	6.36/24.2	1.5	
12	βB3-crystallin	XP_001929508	266	6.36/24.2	1.5	
13	βB2-crystallin	XP_001924958	112	6.45/23.3	0.9	
14	βA2-crystallin	NP_776949	262	6.15/22.2	3.1	
15	βB2-crystallin	XP_001924958	534	6.45/23.3	9.4	
16	βB3-crystallin	XP_001929508	658	6.36/24.2	2.8	
17	βB2 -crystallin	XP_001924958	321	6.45/23.3	5.5	
18	βB2 -crystallin	XP_001924958	390	6.45/23.3	0.9	
19	βB2 -crystallin	XP_001924958	193	6.45/23.3	1.4	
20	βA4 -crystallin	XP_001927427	206	5.91/22.4	1.3	

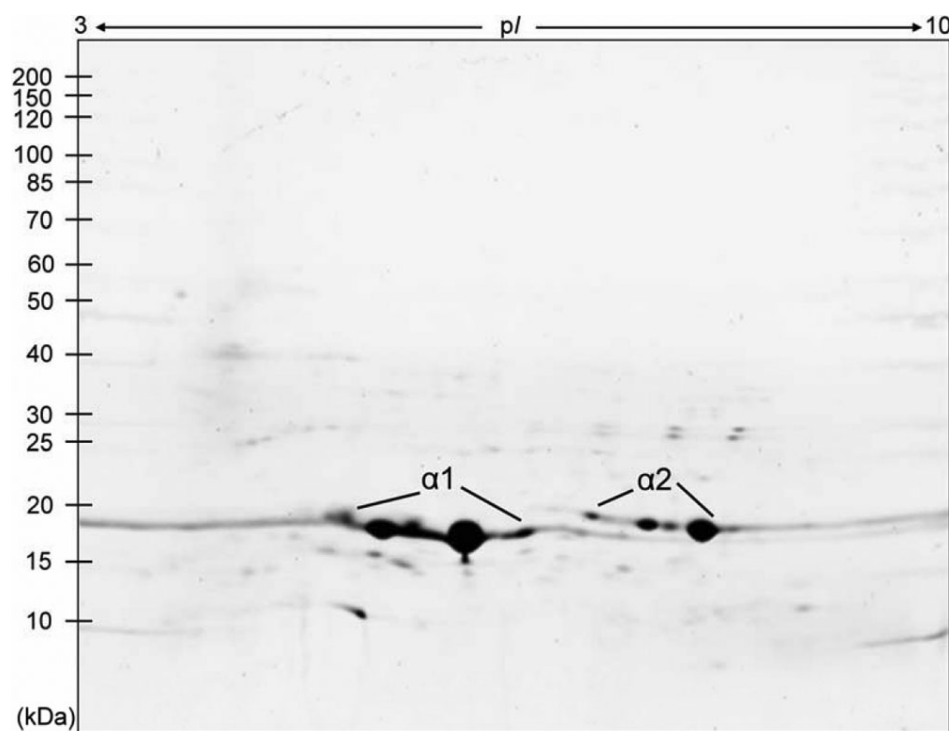In the "Phosphopeptides" column, the phosphorylation sites are underlined.

Figure 2. 2-DE gel patterns of αA- and αB-crystallins in a porcine lens. After purification of α-crystallin by gel filtration according to our previous report [5], 100 μg α-crystallin was loaded onto IPG gel strips (pH 3–10 Nonlinear, 13 cm). The IPG strips were rehydrated, and after IEF, subjected to 2-DE. Protein spots marked and enclosed by α1 and α2 on the map denote the acidic αA-crystallin and basic αB-crystallin subunits of native α-crystallin, respectively. They were further digested by trypsin and identified by nano LC-MS/MS. It is noted that only αB-crystallin spots were found to be phosphorylated by gel-based 2-DE proteomic analysis.

first-dimension IEF strips was 3–10 and the second-dimension SDS–PAGE was run at 12.5% polyacrylamide gel (Figure 1). The proteomic analysis showed that most lens proteins located on the basic and low molecular weight regions correspond to lens crystallins (protein spots No. 1–20) as revealed by LC-MS/MS (Table 1). In our analysis, seven protein spots located on the acidic and basic region on 2D gel were identified as αA-crystallin (protein spots No. 1–4) and αB-crystallin (protein spot No. 5–7), respectively. We also detected 13 protein spots that belong to the class of β-crystallin (protein spots No. 8–20).
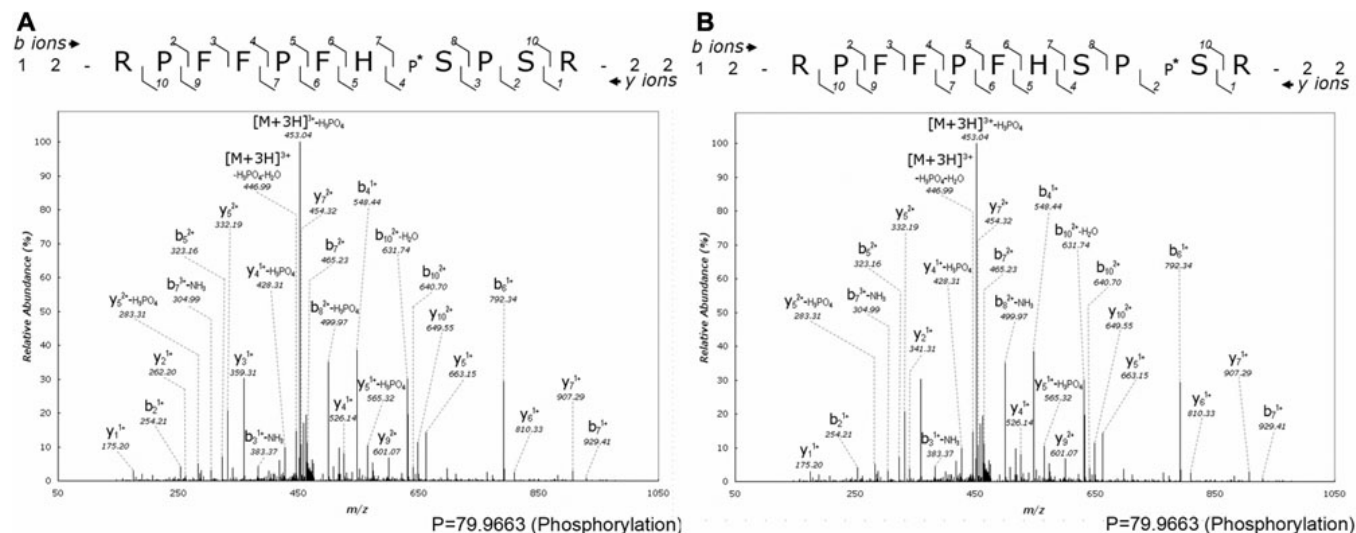
Figure 3. The representative tandem mass spectra of the phosphorylated peptides [12]RPFFPFHS*PSR[22] and [12]RPFFPFHSPS*R[22]. **A**: MS/MS spectrum of the peptide phosphorylated at Ser-19. **B**: MS/MS spectrum of the peptide phosphorylated at Ser-21. The purified phosphopeptides samples less than 1 μg each from IMAC were first injected into a 2 cm×180 μm capillary trap column followed by LC-MS/MS and spectra collection. Based on the tandem mass spectra of the modified peptides [12]RPFFPFHS*PSR[22] and [12]RPFFPFHSPS*R[22] as compared with the original peptide, it can be deduced that either Ser-19 or Ser-21 is phosphorylated. The location of the peptide fragment within the protein is shown by the residue numbers 12 and 22 for the NH$_2$- and COOH-terminus of the phosphorylated peptide sequence. Identified b- and y-ion fragment series are marked by the numbers above and under the peptide sequence, respectively. The putative site of phosphorylation is indicated by * and P* next to serine residues. The mass signals were amplified fivefold, except the ion with the highest intensity.

To further characterize whether the proteins in porcine lens were phosphorylated, we enriched the phosphorylated peptides by performing IMAC protocol followed by phosphorylation site identification with LC-MS/MS. As shown in Table 1, the MS/MS data indicated that either Ser-19 or Ser-21 of the peptide RPFFPFHS[19]PS[21]R in αB-crystallin was phosphorylated. However, we could not find any phosphopeptides in trypsin-digested protein spots corresponding to other lens proteins when using the 2-DE approach.

Gel-based proteomic analysis of phosphorylated αB-crystallin: Because αB-crystallin is the only phosphorylated crystallin in the global protein-expression profile of total porcine lens proteins, we further confirmed the phosphorylation site of αB-crystallin by isolation and purification of α-crystallin on native gel-filtration chromatography of total lens extract [5], followed by 2-DE and LC-MS/MS analysis. As shown in Figure 2, αB-crystallin spots (marked as α2) were located in the basic region, in contrast to αA-crystallin spots (marked as α1) in the acidic side of the gel. After LC-MS/MS analysis of these protein spots, the same phosphorylated peptides [12]RPFFPFHS*PSR[22] and [12]RPFFPFHSPS*R[22] present in αB-crystallin were found (Figure 3). Therefore, we demonstrated that phosphorylation sites at Ser-19 and Ser-21 in αB-crystallin were indeed identified and confirmed by gel-based proteomic analysis.

Gel-free proteomic analysis of phosphorylated proteins in porcine lens: Because the capability of a gel-based proteomic approach to identify phosphoproteins was limited for phosphoprotein identification, we adopted instead for a gel-free protocol similar to shotgun proteomic approaches [11,12]. By enrichment of the porcine lens phosphopeptides on IMAC followed by LC-MS/MS analysis, we have identified 195 phosphopeptides. Among the identified phosphopeptides, the proportions of phosphorylation on serine or threonine in the porcine lens were 85% and 15% (data not shown), respectively. As shown in Table 2, the 27 nondegenerate phosphopeptides belonged to six proteins in the porcine lens, including αB-crystallin, αA-crystallin, βB1-crystallin, β-enolase, heat shock protein β-1 (HSP27), and glucose-6-phosphate isomerase (GPI).

In contrast to traditional gel-based proteomic analysis, the gel-free methods can analyze all compositions of phosphopeptides in the porcine lens. As shown in Figure 4A, most phosphopeptides were identified from αB-crystallin, indicating that it is probably the most abundant phosphoprotein in the porcine lens tissue. The proportion of other phosphopeptides identified in αA-crystallin, βB1-crystallin, β-enolase, HSP27 and GPI were 14%, 11%, 6%, 3%, and 2%, respectively, emphasizing the fact that α-crystallin consisting of αA- and αB-crystallin subunits is indeed the major phosphorylation target in the lens and may play a significant role in the phosphorylation-related biosignaling function of transparent lenses.

Identification of phosphorylation sites in lens crystallins: As shown in Table 2, the phosphorylation sites of αA-crystallin, αB-crystallin, and βB1-crystallin were found to spread over the entire polypeptide regions of these three crystallins. Based on the proportion of phosphorylation sites

TABLE 2. SUMMARY OF IDENTIFIED PHOSPHORYLATED PROTEINS AND PHOSPHORYLATED SITES IN PORCINE LENS PROTEINS BY IMAC FOLLOWED BY LC-MS/MS ANALYSIS.

Protein [Accession number]	Fragment	Phosphopeptides	Designation
αB-crystallin	12–22	RPFFPFHSPSR	Ser-19
[Q7M2W6]	12–22	RPFFPFHSPSR	Ser-21
	57–69	APSWIDTGLSEMR	Ser-59
	57–69	APSWIDTGLSEMR	Thr-63
	73–82	DRFSVNLDVK	Ser-76
	124–149	IPADVDPLTITSSLSSDGVLTVNGPR	Ser-139
	164–174	EEKPAVTAAPK	Thr-170
αA-crystallin	13–21	ALGPFYPSR	Ser-20
[P02475]	55–65	TVLDSGVSEVR	Ser-59
	55–65	TVLDSGVSEVR	Ser-62
	55–70	TVLDSGVSEVRSDRDK	Ser-66
	79–88	HFSPEDLTVK	Ser-81
	79–88	HFSPEDLTVK	Thr-86
	146–157	VPSGVDAGHSER	Ser-148
	146–157	VPSGVDAGHSER	Ser-155
	158–173	AIPVSREEKPSSAPTS	Ser-173
Beta-crystallin B1	8–21	ASATAAVNPGPDGK	Ser-9
[Q007T1]	8–21	ASATAAVNPGPDGK	Ser-11
	88–107	VRSIIVTSGPWVAFEQSNFR	Ser-90
	90–107	SIIVTSGPWVAFEQSNFR	Ser-95
	185–199	VSSGTWVGYQYPGYR	Thr-189
Beta-enolase	81–89	KLSVVDQEK	Ser-83
[Q1KYT0]	257–269	YDLDFKSPDDPSR	Ser-263
Heat shock protein beta-1	13–20	SPSWDPFR	Ser-13
[Q5S1U1]	13–20	SPSWDPFR	Ser-15
Glucose-6-phosphate isomerase	227–241	EWFLQSAKDPSAVAK	Ser-232
[NP_999495]	448–461	ELQAAGKSPEDFEK	Ser-455

In the "Phosphopeptides" column, the phosphorylation sites are underlined.

in each crystallin, we found that Ser-59 and Thr-189 are two predominant phosphorylation-sites in αB-crystallin and βB1-crystallin, respectively (Figure 4B,C). To our knowledge, phosphorylation at Thr-189 of βB1-crystallin identified in this study is a new and first-reported phosphorylation site for β-crystallin class of lens crystallins. In addition, nine phosphorylated sites of αA-crystallin were found to distribute more or less evenly on the whole polypeptide chain with the exception of Ser-155, Ser-81, and Ser-59 (Figure 4D). In contrast the phosphorylation of αB-crystallin was shown to distribute unevenly over the whole crystallin with the highest proportion of phosphorylation occurring at Ser-59 followed by Ser-19 (Figure 4B). The mechanisms that account for the different extents of phosphorylation at specific sites of αA- and αB-crystallins remain unknown and is to be investigated in the future.

Identification of phosphorylation sites in β-enolase, glucose-6-phosphate isomerase (GPI), and heat shock protein β-1 (HSP 27): In addition to lens crystallins, three non-crystallin proteins were also found to be phosphorylated in vivo in our proteomic analysis (Table 2). The β-enolase was found to be phosphorylated at Ser-83 and Ser-263 and GPI phosphorylated at Ser-232 and Ser-455. It is noteworthy that similar to αB-crystallin, a member of the heat shock protein

family, a lenticular HSP27 with chaperone activity was shown to be phosphorylated at Ser-13 and Ser-15.

Conclusions: Besides αA- and αB-crystallins which show chaperone activity and extensive phosphorylation, βB1-crystallin and non-crystallin cellular proteins, such as β-enolase, heat shock protein β-1 (HSP27), and glucose-6-phosphate isomerase have also been shown for the first time to be phosphorylated in vivo at specific sites. Moreover, αA- and αB-crystallins were found to be the most abundantly phosphorylated proteins in porcine lenses, being exclusively phosphorylated on serine or threonine but not on tyrosine residues. Using the gel-free proteomic strategy by employing IMAC enrichment of phosphopeptides from a trypsin-digested lens protein mixture followed by sensitive LC-MS/MS proves to be superior to conventional proteomic analysis based on the pre-MS/MS 2-DE separation of protein samples. The improved strategy of gel-free phosphoproteomics analysis affords a more effective and facile method for the determination of in vivo phosphorylation sites of whole tissue extract. The use of site-directed mutagenic substitution of Asp for the phosphorylated sites of Ser or Thr residues to mimic the phosphorylation status of chaperoning αA- or αB-crystallin [27-30] will help elucidate the role of
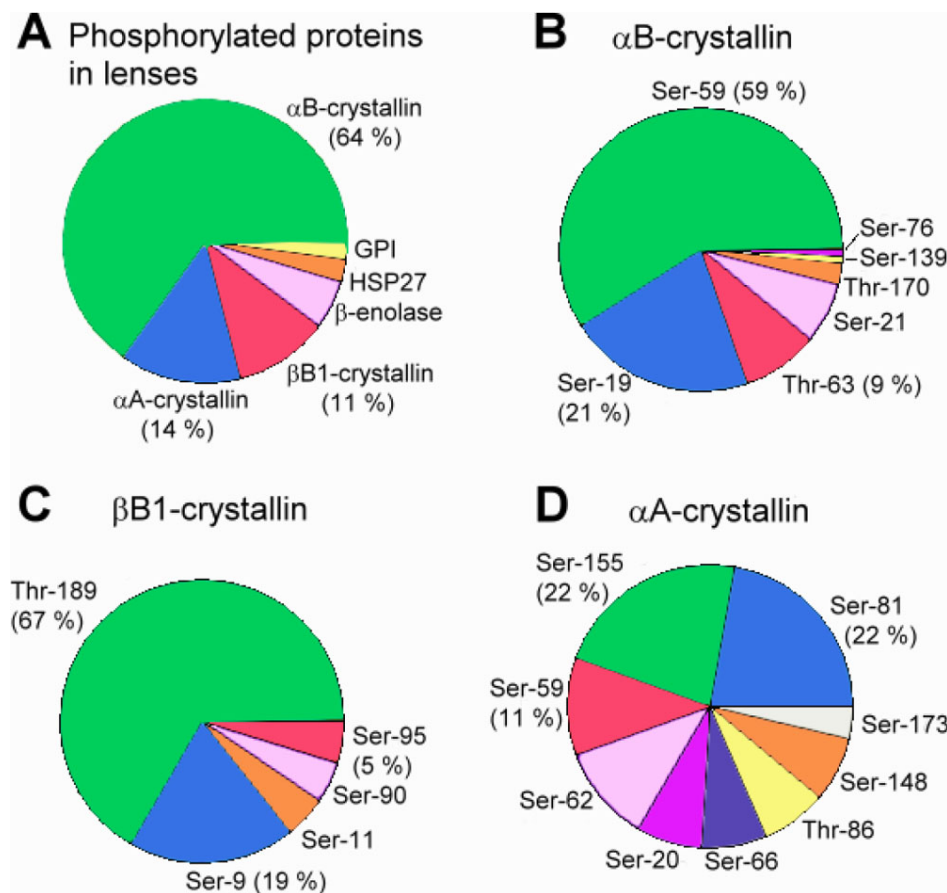
Figure 4. The percent distribution of phosphorylated sites identified by gel-free IMAC enriched phosphopeptide and LC-MS/MS analysis. **A**: Proportion of the proteins with phosphorylation in total lens extract. **B**: Distribution of in vivo phosphorylation sites in αB-crystallin. **C**: Distribution of in vivo phosphorylation sites in βB1-crystallin. **D**: Distribution of in vivo phosphorylation sites in αA-crystallin. The three most abundantly phosphorylated proteins (%) in the lens are shown under the identified phosphoproteins in **A-D**. It is noted that phosphorylated sites of αA-crystallin are more evenly distributed along the protein molecule than αB- and βB1-crystallins which show the predominant phosphorylation sites at residues 59 and 189 in αB- and βB1-crystallins, respectively.

phosphorylation in relation to the chaperone-like activity and their biological significance [25,31,32].

REFERENCES

1. Harding JJ, Dilley KJ. Structural proteins of the mammalian lens: a review with emphasis on changes in development, aging and cataract. Exp Eye Res 1976; 22:1-73. [PMID: 767125]

2. de Jong WW, Hendriks W, Mulders JW, Bloemendal H. Evolution of eye lens crystallins: the stress connection. Trends Biochem Sci 1989; 14:365-8. [PMID: 2688200]

3. Van Kleef FS, De Jong WW, Hoenders HJ. Stepwise degradations and deamidation of the eye lens protein alpha-crystallin in ageing. Nature 1975; 258:264-6. [PMID: 1202360]

4. Miesbauer LR, Zhou X, Yang Z, Sun Y, Smith DL, Smith JB. Post-translational modifications of water-soluble human lens crystallins from young adults. J Biol Chem 1994; 269:12494-502. [PMID: 8175657]

5. Liao JH, Lee JS, Wu SH, Chiou SH. COOH-terminal truncations and site-directed mutations enhance thermostability and chaperone-like activity of porcine alphaB-crystallin. Mol Vis 2009; 15:1429-44. [PMID: 19641632]

6. Pawson T, Scott JD. Signaling through scaffold, anchoring, and adaptor proteins. Science 1997; 278:2075-80. [PMID: 9405336]

7. MacCoss MJ, McDonald WH, Saraf A, Sadygov R, Clark JM, Tasto JJ, Gould KL, Wolters D, Washburn M, Weiss A, Clark JI, Yates JR 3rd. Shotgun identification of protein modifications from protein complexes and lens tissue. Proc Natl Acad Sci USA 2002; 99:7900-5. [PMID: 12060738]

8. Chiou SH, Wu SH. Evaluation of commonly used electrophoretic methods for the analysis of proteins and peptides and their application to biotechnology. Anal Chim Acta 1999; 383:47-60.

9. Han CL, Chien CW, Chen WC, Chen YR, Wu CP, Li H, Chen YJ. A multiplexed quantitative strategy for membrane proteomics: opportunities for mining therapeutic targets for autosomal dominant polycystic kidney disease. Mol Cell Proteomics 2008; 7:1983-97. [PMID: 18490355]

10. Ong SE, Blagoev B, Kratchmarova I, Kristensen DB, Steen H, Pandey A, Mann M. Stable isotope labeling by amino acids in cell culture, SILAC, as a simple and accurate approach to expression proteomics. Mol Cell Proteomics 2002; 1:376-86. [PMID: 12118079]

11. McCormack AL, Schieltz DM, Goode B, Yang S, Barnes G, Drubin D, Yates JR 3rd. Direct analysis and identification of

proteins in mixtures by LC/MS/MS and database searching at the low-femtomole level. Anal Chem 1997; 69:767-76. [PMID: 9043199]

12. Washburn MP, Wolters D, Yates JR 3rd. Large-scale analysis of the yeast proteome by multidimensional protein identification technology. Nat Biotechnol 2001; 19:242-7. [PMID: 11231557]

13. Chiou SH, Azari P, Himmel ME, Squire PG. Isolation and physical characterization of bovine lens crystallins. Int J Pept Protein Res 1979; 13:409-17. [PMID: 457334]

14. Chiou SH, Chylack LT Jr, Tung WH, Bunn HF. Nonenzymatic glycosylation of bovine lens crystallins. Effect of aging. J Biol Chem 1981; 256:5176-80. [PMID: 7228874]

15. Liao JH, Hung CC, Lee JS, Wu SH, Chiou SH. Characterization, cloning, and expression of porcine alpha B crystallin. Biochem Biophys Res Commun 1998; 244:131-7. [PMID: 9514893]

16. Lee JS, Samejima T, Liao JH, Wu SH, Chiou SH. Physiological role of the association complexes of alpha-crystallin and its substrates on the chaperone activity. Biochem Biophys Res Commun 1998; 244:379-83. [PMID: 9514930]

17. Liao JH, Lee JS, Chiou SH. Distinct roles of alphaA- and alphaB-crystallins under thermal and UV stresses. Biochem Biophys Res Commun 2002; 295:854-61. [PMID: 12127973]

18. Lu X, Zhu H. Tube-gel digestion: a novel proteomic approach for high throughput analysis of membrane proteins. Mol Cell Proteomics 2005; 4:1948-58. [PMID: 16150870]

19. Tsai CF, Wang YT, Chen YR, Lai CY, Lin PY, Pan KT, Chen JY, Khoo KH, Chen YJ. Immobilized metal affinity chromatography revisited: pH/acid control toward high selectivity in phosphoproteomics. J Proteome Res 2008; 7:4058-69. [PMID: 18707149]

20. Ideker T, Thorsson V, Ranish JA, Christmas R, Buhler J, Eng JK, Bumgarner R, Goodlett DR, Aebersold R, Hood L. Integrated genomic and proteomic analyses of a systematically perturbed metabolic network. Science 2001; 292:929-34. [PMID: 11340206]

21. Zhou H, Watts JD, Aebersold R. A systematic approach to the analysis of protein phosphorylation. Nat Biotechnol 2001; 19:375-8. [PMID: 11283598]

22. Spector A, Chiesa R, Sredy J, Garner W. cAMP-dependent phosphorylation of bovine lens alpha-crystallin. Proc Natl Acad Sci USA 1985; 82:4712-6. [PMID: 2991889]

23. Chiesa R, Gawinowicz-Kolks MA, Kleiman NJ, Spector A. Definition and comparison of the phosphorylation sites of the A and B chains of bovine alpha-crystallin. Exp Eye Res 1988; 46:199-208. [PMID: 3350065]

24. Voorter CE, de Haard-Hoekman WA, Roersma ES, Meyer HE, Bloemendal H, de Jong WW. The in vivo phosphorylation sites of bovine alpha B-crystallin. FEBS Lett 1989; 259:50-2. [PMID: 2599111]

25. Aquilina JA, Benesch JL, Ding LL, Yaron O, Horwitz J, Robinson CV. Phosphorylation of alphaB-crystallin alters chaperone function through loss of dimeric substructure. J Biol Chem 2004; 279:28675-80. [PMID: 15117944]

26. Smith JB, Thevenon-Emeric G, Smith DL, Green B. Elucidation of the primary structures of proteins by mass spectrometry. Anal Biochem 1991; 193:118-24. [PMID: 2042736]

27. Nicholl ID, Quinlan RA. Chaperone activity of alpha-crystallins modulates intermediate filament assembly. EMBO J 1994; 13:945-53. [PMID: 7906647]

28. Kamei A, Hamaguchi T, Matsuura N, Masuda K. Does post-translational modification influence chaperone-like activity of alpha-crystallin? I. Study on phosphorylation. Biol Pharm Bull 2001; 24:96-9. [PMID: 11201254]

29. Moroni M, Garland D. In vitro dephosphorylation of alpha-crystallin is dependent on the state of oligomerization. Biochim Biophys Acta 2001; 1546:282-90. [PMID: 11295434]

30. Ito H, Kamei K, Iwamoto I, Inaguma Y, Nohara D, Kato K. Phosphorylation-induced change of the oligomerization state of alpha B-crystallin. J Biol Chem 2001; 276:5346-52. [PMID: 11096101]

31. Ahmad MF, Raman B, Ramakrishna T, Rao Ch M. Effect of phosphorylation on alpha B-crystallin: differences in stability, subunit exchange and chaperone activity of homo and mixed oligomers of alpha B-crystallin and its phosphorylation-mimicking mutant. J Mol Biol 2008; 375:1040-51. [PMID: 18061612]

32. Aggeli IK, Beis I, Gaitanaki C. Oxidative stress and calpain inhibition induce alpha B-crystallin phosphorylation via p38-MAPK and calcium signalling pathways in H9c2 cells. Cell Signal 2008; 20:1292-302. [PMID: 18420382]